An output coupler for a W-band high power wideband gyro-amplifier

Paul McElhinney, Craig R. Donaldson, Johannes E. McKay, Liang Zhang, Duncan A. Robertson, *Member IEEE*, Robert I. Hunter, Graham M. Smith, Wenlong He and Adrian W. Cross

***Abstract*—An output coupler for a W-band high power wideband gyro-amplifier has been designed, manufactured and experimentally measured. It consists of a high performance $\sin^2$-parallel corrugated horn integrated with a broadband multi-layer window. The major design requirements are that the horn/window combination must have an input return loss lower than -30 dB over a 10 GHz bandwidth, provide a high quality output beam pattern, and operate under ultra-high vacuum conditions. The coupler converts a circular waveguide TE_{11} mode into the free space Laguerre Gaussian LG_{00} mode over the frequency band of 90–100 GHz with a measured return loss of between -30 and -40 dB and a simulated Gaussian coupling efficiency of over 99% at 94 GHz.**

***Index Terms*—corrugated horn, Gaussian coupling, microwave window**

I. Introduction

Gyro-devices [1-3] are well suited to applications in plasma physics, remote sensing, radar, high-field electron paramagnetic resonance and dynamic nuclear polarization for nuclear magnetic resonance due to their capability to produce high power coherent radiation at high frequencies in the millimeter and sub-millimeter range. A W-band gyrotron backward wave oscillator (gyro-BWO) [4] and gyrotron traveling wave amplifier (gyro-TWA) based on a cusp electron beam source [5, 6] have been developed to provide a wideband tunable source with an output power of ~10 kW and ~5 kW, respectively. The gyro-TWA is designed to amplify a 1 W signal, injected through an input coupler [7, 8], to a power of ~5 kW over the frequency range of 90-100 GHz. The gyro-TWA uses a helically corrugated interaction region to allow high power amplification over a broadband frequency range. The input and output mode of the interaction region is a circularly polarized TE_{11} mode whilst the interaction is at the 2^{nd} harmonic of the electron cyclotron frequency. The amplified signal is then output though a corrugated horn [9] and a multi-layer vacuum window [10, 11] to provide a high purity Gaussian beam, suitable for many applications.

The output coupler needs to operate under ultra-high vacuum (UHV) conditions and ideally have a reflection coefficient of less than -30 dB across the 10 GHz bandwidth of the amplifier to avoid the possibility of parasitic oscillations. For most applications it is also desirable for the output beam to have as low sidelobes as possible to minimize uncoupled or scattered power.

Previously, the horn and window were designed and manufactured as separate components. The original corrugated horn [9] had a 105 mm long $\sin^2$ profile over which the corrugation depth tapered linearly from ~$\lambda/2$ to $\lambda/4$ to minimize the reflection over the operational bandwidth. The input and output radii were 2.8 and 13.0 mm respectively. That horn achieved an input reflection coefficient of better than -30 dB over a 10 GHz bandwidth, a Gaussian coupling efficiency of 98% at band center, and sidelobe levels at -25 dB. The original window [10, 11] used a 3-disk multi-layer configuration in which performance was optimized when the phase front of the incident beam was planar at the vacuum window and field components were kept away from the edges of the window. That horn and window combination achieved an input return loss of better than -27 dB over 90-100 GHz.

This work describes a new integrated horn and window output coupler, designed to interface with a quasi-optical transmission line suitable for integration into radar or magnetic resonance spectroscopy applications. The new design aims to achieve higher performance by combining HE_{1n} modes in phase at the aperture [12]. The primary objectives were to maximize the Gaussian coupling and reduce the sidelobe levels, to maximize power delivery to the application and minimize scattered power, whilst maintaining the low input return loss to ensure amplifier stability with high gain interaction regions, within a vacuum compatible construction.

In this paper, the design, manufacture and measurement of the new UHV-compatible integrated corrugated horn and window are presented.

II. Simulation and Optimization of the Horn and Window

The corrugated horn antenna has been extensively studied and reported by Clarricoats [13] for radar and communications applications. The corrugated horn primarily converts the TE_{11} input waveguide mode into the HE_{11} corrugated horn mode, which has an aperture electric field distribution of the form given by Eq. 1

This work was supported by the Engineering and Physical Sciences Research Council (EPSRC) U.K. under Research Grant EP/K029746/1, and Science and Technology Facilities Council (STFC) U.K. under Research Grants ST/K006673/1 & ST/K006703/1, ST/N002326/1 & ST/N002318/1.

Paul McElhinney (paul.mcelhinney@strath.ac.uk), C. R. Donaldson (craig.donaldson@strath.ac.uk), L. Zhang (liang.zhang@strath.ac.uk), W. He (w.he@strath.ac.uk), and A. W. Cross (a.w.cross@strath.ac.uk) are with Department of Physics, SUPA, University of Strathclyde Glasgow, G4 0NG, Scotland. J.E. McKay is now with the National High Magnetic Field Laboratory (NHMFL) Tallahassee, FL USA (mckay@magnet.fsu.edu). D.A. Robertson (dar@st-and.ac.uk), R.I. Hunter (rih1@st-and.ac.uk) and G.M. Smith (gms@st-and.ac.uk) are with the SUPA, School of Physics & Astronomy, University of St Andrews, KY16 9SS, Scotland.

Manuscript received MMMM DD, YYYY; revised MMMM DD, YYYY.

$$E_r(r) = J_0\left(\frac{2.405\, r}{a_0}\right) \quad (1)$$

where a_0 is the radius of the aperture, r is the radius and J_0 is the zeroth order Bessel function of the first kind. This aperture field is close to a Gaussian field distribution and it has been shown that a pure HE_{11} mode will couple with 98% efficiency to a fundamental Laguerre Gaussian LG_{00} beam with a beam waist $\omega_0 = 0.644/a_0$ situated at the aperture [14, 15].

In practice any corrugated horn taper will also excite higher order HE_{1n} modes and in particular the HE_{12} mode. The relative magnitude and phasing of this mode, with respect to the HE_{11} mode, is the main factor that determines the amplitude and effective radius of curvature of the field at the aperture [16]. This in turn determines the coupling coefficients to any given orthonormal Gaussian mode beam set, specified by a fundamental beam radius ω and radius of curvature R, at the aperture.

It can be shown to a good approximation that coupling to a fundamental Gaussian beam, with a planar wavefront, is maximized when the HE_{12} mode is in phase with the HE_{11} mode and the respective amplitude levels are approximately 0.2 and 0.98 [12]. For this particular case the beam waist will be situated close to the aperture with a radius $\omega_0 \approx 0.57a_0$.

The profile of the new horn, consists of a $\sin^2$ corrugated profile to excite the desired HE_{12} amplitude, followed by a straight corrugated phasing section to bring the modes into phase at the aperture, a design which has been described previously [12, 18]. The $\sin^2$ profile can be described by Eq. 2

$$r(z) = r_{in} + (r_{out} - r_{in})\left[\frac{Z}{L}(1-A) + A\sin^2\left(\frac{\pi z}{2L}\right)\right] \quad (2)$$

where L, r_{in} and r_{out} are the length, the input and output radius of the profiled section. The value of A approximately determines how much of the HE_{12} mode is excited [12].

Simulations show that a value of A ~ 0.7 excites the desired 0.2 HE_{12} amplitude (4% power) and leads to respective lengths for the $\sin^2$ profile and linear phasing section of:

$$L_{horn} = L_{profile} + L_{phase} = \frac{2.4a_0^2}{\lambda_0} + \frac{2a_0^2}{\lambda_0} \quad (3)$$

where λ_0 is the free space wavelength at the desired frequency f_0, and a_0 is the output aperture radius. The input radius r_{in} of 1.45 mm matches that of the output radius of the gyro-TWA interaction region. The output radius r_{out} of 12.5 mm was chosen for practical reasons relating to fragility of the window components and keeping the horn length reasonable. From these values it is possible to derive an approximate initial length of the profiled section and that of the phase matching section using Eq. 3.

The design of the throat of the horn was optimized to minimize the input return loss. The depth of the input corrugations was tapered from close to the nominal λ/2 value to λ/4 over an impedance matching section of 20 corrugations. The gap and vane thicknesses were set to 0.5 and 0.3 mm respectively.

The window section is composed of a series of dielectric disks and gaps with stepped radii, as shown in Fig. 1. The fused quartz disks (a) and the ceramic disk (b) are similar to the previous multi-layer window design, which operated on the TE_{11} output mode [10]. In addition to the stepped structure of the vacuum window there are two retaining rings (c) and thin copper rings (d) as well as corrugation gaps and vanes (e, f). The retaining rings and copper rings were used to achieve the exact gap spacing between the quartz disks (a) and the ceramic disk (b). The corrugations in the window region are of the same depth and pitch as those in the phase matching section of the corrugated horn. Details of the optimized and constructed window structure can be found in Table I and also [10].

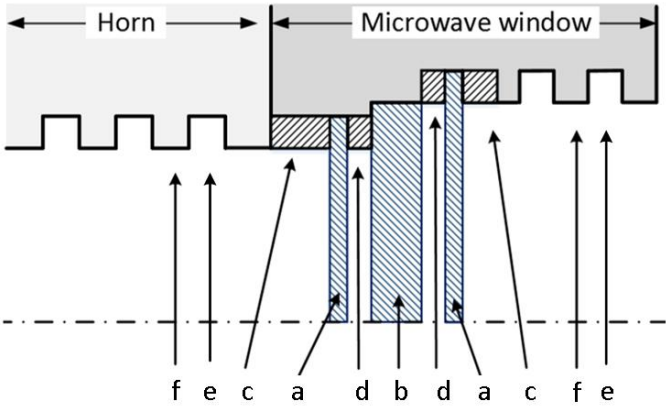

Fig. 1. Schematic of the horn/window assembly. Quartz disks (a), ceramic disk (b), retaining rings (c), copper rings (d) and corrugation gaps (e) and vanes (f).

TABLE I
MICROWAVE WINDOW PROPERTIES

Section	Length (mm)	Permittivity (ε_r)
a	0.20	3.75
b	1.61	9.4
c	1.00	1
d	0.19	1
e	0.30	1
f	0.50	1

The structures of the corrugated horn, the phase matching section and the window are rotationally symmetric, making mode matching analysis particularly suitable. Initially, both CORRUG [18] and μ-wave Wizard [19] were used to calculate scattering parameters and aperture fields of the horn alone from which far-field patterns and coupling coefficients to the desired Gaussian mode set could be calculated. Both programs gave equivalent results.

Once the initial baseline design of the horn was defined, μ-wave Wizard was used for optimization of the full structure including the window components as it is capable of simulating dielectric sections which is not possible with CORRUG. The optimization parameters were the phase matching section length L_{phase} and the impedance matching corrugation depths as well as the dimensions of the multilayer window sections

(a)-(d). Finally, the whole structure was simulated in CST Microwave Studio [20] which confirmed the mode-matching predictions.

The resulting design is predicted to have a beam waist at the aperture of $\omega_0 = 6.81$ mm or $0.54a_0$ The coupling between the aperture field and the fundamental Gaussian free-space mode was calculated to be 99.4% at 94 GHz, 99.2% at 90 GHz and 98.5% at 100 GHz. These values are close to the theoretical maximum obtainable of 99.6% for $\omega_0 \approx 0.57a_0$ [12].

III. Construction and Assembly

The construction of the horn was carried out by Thomas Keating Ltd. using an electroforming process. During this stage, two ultra-high vacuum flanges are attached to the horn by growing copper over the spigot flanges to form a tight seal. The aluminum is then dissolved leaving the finished horn. The window consists of an alumina disk that is vacuum brazed into a titanium jacket that contains the knife edge to seal the vacuum. This assembly sits inside a stainless ring with through holes to connect to the corrugated horn. Fig. 2 shows a photograph of the finished horn and the window assembly. The total length of the horn and window is 233.8 mm.

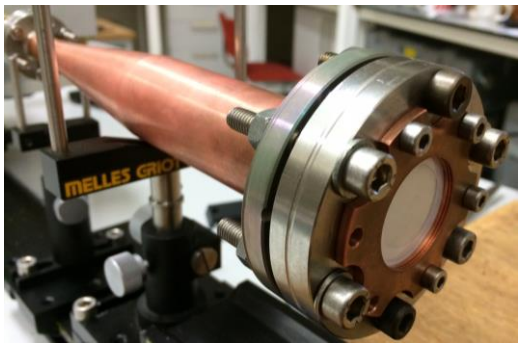

Fig.2. Photo of the constructed horn and window assembly.

The soft copper spacing rings that are between each quartz disk, and the central alumina disk allow for fine tuning of the window to compensate for manufacturing tolerances of the components as well as environmental conditions, which may induce a deviation from the ideal simulated design. The adjustment is carried out whilst measuring the return loss on a vector network analyzer (VNA): the scattering parameters can be fine-tuned to match those of the simulations. The final assembly was leak tested and was able to hold the vacuum to 10^{-9} mbar.

IV. Experimental Results

Reflection and far- and near-field antenna measurements of the horn prototype were measured using a W-band VNA (Anritsu ME7808B). In order to measure the reflection of the horn and horn-window assembly a rectangular-to-circular converter and a circular taper were used to connect an output port of the VNA to the horn.

Experimental results and simulated predictions for the input reflection of the horn and the horn and window combination are shown in Fig. 3. The reflection remains below -30 dB over 91 to 100 GHz and is better than -40 dB at 94 GHz. It should be noted that the differences between the measured and the simulated reflections in Fig. 3 are due to the addition of the rectangular to circular converter and the circular taper. The simulations and measurements also show a small amount of modes which were trapped between the horn and the window. In this design the radius of the window was chosen to be large enough to reduce the trapped mode to a level of lower than -35 dB.

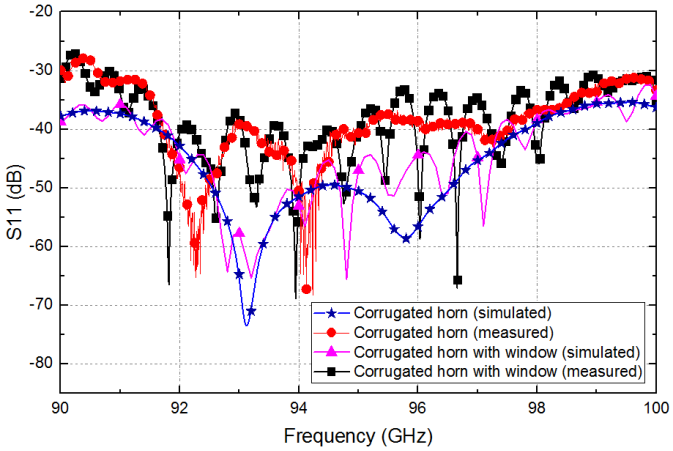

Fig. 3. Microwave reflection measurement and simulation of the corrugated horn with and without the window in place.

Far-field radiation measurements of the co-polar E-plane, H-plane and the cross-polar D-plane components were also carried out at 94 GHz, with the window in place, and are shown in Fig. 4. Low sidelobe levels of -35 dB are in excellent agreement with simulations of the horn alone and demonstrate that the addition of the window has a negligible effect on the antenna pattern. The cross-polar measurement is also in good agreement with the simulations, with a maximum of -31.8 dB, compared to a simulated maximum of -34.2 dB.

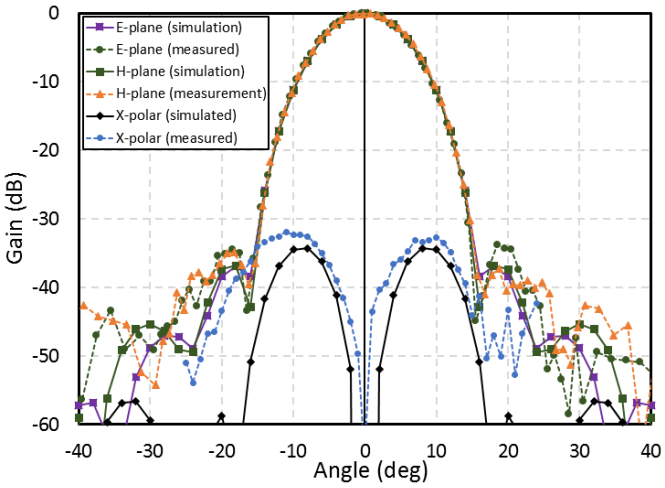

Fig 4. The measured and simulated co-polar E-plane, H-plane and cross-polar D-plane scans of the output coupler with window at 94 GHz.

A quick planar near field scan was also carried out using a WR-10 waveguide probe which was mounted on the second port of the VNA and scanned across the aperture of the horn with the window in place at a distance of 10 mm from the aperture. The transmission coefficient S_{21} was recorded. Fig. 5 shows the normalized aperture field intensity from the measurement. It is believed that standing waves between the

window and the measurement probe and surrounding hardware are the cause of the intensity fluctuations in the measurement which degrade the beam symmetry.

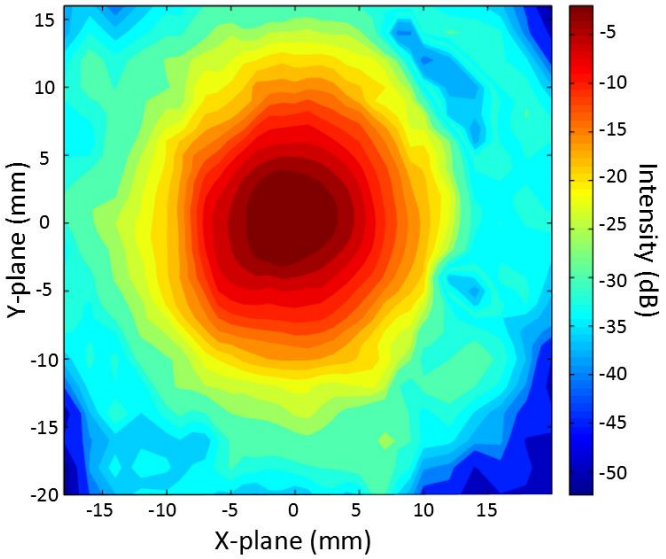

Fig. 5. Planar near field normalized intensity plot measured at 10 mm from the window aperture.

V. CONCLUSIONS

Using a mixture of analytical and computational methods, we have shown it is possible to design and construct an output coupler, comprising an integrated horn and a multi-layer window, which is capable of being incorporated into a wideband gyro-TWA operating under UHV conditions. The excellent agreement between simulation and the experimentally measured far field pattern indicates that the window has not created new modes within the antenna. The predicted Gaussian coupling efficiency is 99.4% and low sidelobe levels of -35 dB were measured at 94 GHz. The input reflection is less than -30 dB over almost the entire 90-100 GHz band and better than -40 dB at 94 GHz. The output coupler holds vacuum to 10^{-9} mbar. This performance represents a significant improvement over previous designs and means the new output coupler is suitable for its intended use in a wideband, high power gyro-TWA, relevant for applications in radar and magnetic resonance spectroscopy.

ACKNOWLEDGEMENT

The authors thank Dr Richard Wylde of Thomas Keating Ltd. for electroforming the horn and grafting on the UHV flanges.

REFERENCES

[1] G. G. Denisov, V. L. Bratman, A. W. Cross, W. He, A.D.R. Phelps, K. Ronald, S.V. Samsonov, and C.G. Whyte, "Gyrotron travelling wave amplifier with a helical interaction waveguide," *Phys. Rev. Lett*. vol. 81, 5680–5683, 1998.

[2] K. R. Chu, "The electron cyclotron maser," *Rev. Mod. Phys*. vol. 76, 489, 2004.

[3] M. Thumm, "State-of-the-Art of High Power Gyro-Devices and Free Electron Masers," KIT Scientific Reports 7693, Update 2014 KIT Scientific Publishing, Karlsruhe, Germany, 2014.

[4] W. He, C. R. Donaldson, L. Zhang, K. Ronald, P. McElhinney, A. W. Cross, "High power wideband gyrotron backward wave oscillator operating towards the terahertz region," *Phys. Rev. Lett.*, vol. 110, 165101, 2013.

[5] W. He, C. G. Whyte, E. G. Rafferty, A. W. Cross, A. D. R. Phelps, K. Ronald, A.R. Young, C.W. Robertson, D.C. Speirs, and D.H. Rowlands, "Axis-encircling electron beam generation using a smooth magnetic cusp for gyrodevices," *Appl. Phys. Lett.* vol. 93, 121501, 2008.

[6] C. R. Donaldson, W. He, A. W. Cross, F. Li, A. D. R. Phelps, L. Zhang, K. Ronald, C.W. Robertson, C.G. Whyte, A.R. Young, "A cusp electron gun for millimeter wave gyro-devices", *Appl. Phys. Lett.*, vol. 96, 141501, 2010.

[7] L. Zhang, W. He, C. R. Donaldson, J. R. Garner, P. McElhinney, and A. W. Cross, "Design and measurement of a broadband sidewall coupler for a W-band gyro-TWA," *IEEE Trans. Microw. Theory Tech.*, vol. 63, pp. 3183-3190, 2015.

[8] J. Garner, L. Zhang, C. R. Donaldson, A. W. Cross, and W. He, "Design study of a fundamental mode input coupler for a 372-GHz gyro-TWA I: rectangular to circular coupling methods," *IEEE Trans. Electron Dev*., vol. 63, pp. 497-503, 2016.

[9] P. McElhinney, C. R. Donaldson, L. Zhang, and W. He, "A high directivity broadband corrugated horn for W-band gyro-devices," *IEEE Trans. Antennas Propag.*, vol. 61, pp. 1453–1456, 2013.

[10] C. R. Donaldson, W. He, L. Zhang, and A. W. Cross, "A W-band multi-layer microwave window for pulsed operation of gyro-devices," *IEEE Microw. Wireless Compon. Lett.*, vol. 23, pp. 237–239, 2013.

[11] C. R. Donaldson, P. McElhinney, L. Zhang, and W. He, "Wide-Band HE_{11} Mode Terahertz Wave Windows for Gyro-Amplifiers," *IEEE Trans. THz Sci. Technol.*, vol. 6, pp. 108-112, 2016.

[12] J. E. McKay, D. A. Robertson, P. A. S. Cruickshank, R. I. Hunter, D.R. Bolton, R.J. Wylde, and G.M. Smith, "Compact Wideband Corrugated Feedhorns With Ultra-Low Sidelobes for Very High Performance Antennas and Quasi-Optical Systems," *IEEE Trans. Antennas Propag.*, vol.61, pp.1714-1721, 2013.

[13] P. J. B. Clarricoats and A. D. Olver, Corrugated Horns for Microwave Antennas. Peregrinus, London, UK, 1984.

[14] A. D. Olver, P. J. B. Clarricoats, A. A. Kishk, and L. Shafai, Microwave Horns and Feeds. Piscataway, NJ, USA: IEEE Press, 1994.

[15] R. J. Wylde and D. H. Martin, "Gaussian beam-mode analysis and phase-centers of corrugated feed horns," *IEEE Trans. Microw. Theory Tech.*, vol. 48, no. 10, pp. 1691–1699, Oct. 1993

[16] E. J. Kowalski, M. A. Shapiro, and R. J. Temkin, "Simple Correctors for Elimination of High-Order Modes in Corrugated Waveguide Transmission Lines". *IEEE Trans. Plasma Sci.*, vol. 42, no.1, pp. 29–37, 2016

[17] P. A. S. Cruickshank, D. R. Bolton, D. A. Robertson, R. J. Wylde, and G. M. Smith, "Reducing standing waves in quasi-optical systems by optimal feedhorn design," Proc. Joint 32nd Int. Conf. Infrared Millimeter Waves 15th Int. Conf. Terahertz Electronics, Cardiff, U.K., Sep. 2007, pp. 922–923.

[18] *CORRUG*, www.smtconsultancies.co.uk

[19] *μ-wave Wizard*, Mician GmbH, 2012. www.mician.com

[20] *Microwave Studio*, CST GmbH, www.cst.com